

RESEARCH PAPER



Hemolysin BL from novel *Bacillus toyonensis* BV-17 induces antitumor activity both in vitro and in vivo

Jiajia Chen¹^{a*}, Shoukui Hu²^{*}, Dengbo Ji¹^a, Zhaoya Gao³^b, Hanyang Wang¹^a, Yong Yang¹^a, Yongkang Chen¹^a, and Jin Gu¹^{a,b,c}

^aKey Laboratory of Carcinogenesis and Translational Research, Ministry of Education, Peking University Cancer Hospital & Institute, Beijing, China; ^bDepartment of Gastrointestinal Surgery, Peking University Shougang Hospital, Beijing, China; ^cPeking-Tsinghua Center for Life Sciences, Beijing, China

ABSTRACT

The gut microbiota plays an important role in cancer development and immunotherapy. Bacterial toxins have enormous antitumor potential due to their cytotoxicity and ability to activate the immune system. Using 16S rRNA gene sequencing, we compared the gut microbiota composition of fecal samples from healthy individuals and patients with colorectal cancer (CRC) and observed that the *genus Bacillus* was common in the healthy donors but was absent in the CRC patients. Further, we isolated a novel *Bacillus toyonensis* BV-17 from the fecal samples of the healthy individuals. Our results showed that the supernatant of the *Bacillus toyonensis* BV-17 cultures could quickly kill various tumor cell lines within minutes in vitro, by causing cell membrane disruption, blebbing, and leakage of cytoplasmic content. Fast protein liquid chromatography (FPLC) and mass spectrometry analysis identified hemolysin BL (HBL) as the effector molecule, which exhibits a different cytotoxicity mechanism compared to previous studies. Intra-tumor injection of low dose HBL inhibited the growth of both treated and untreated tumors in mice. The outcomes of this pioneer study suggest that HBL exhibits antitumor activity and is a potential chemotherapeutic agent that could be engineered to target only tumor cells in future.

ARTICLE HISTORY

Received 30 April 2020
Revised 28 May 2020
Accepted 5 June 2020

KEYWORDS

Gut microbiota; colorectal cancer; *Bacillus toyonensis* BV-17; hemolysin BL; antitumor activity



Introduction

Cancer is a leading cause of death among the global noncommunicable diseases. Conventional cancer therapies mainly include surgical excision, radiotherapy, and chemotherapy. Unfortunately, cancer recurrence, metastasis, and chemotherapy- or radiotherapy-resistance severely limits treatment efficacy. As such, there is a tremendous need to find new antitumor drugs for advanced cancer patients.


As a common gastrointestinal cancer, colorectal cancer (CRC) ranks third in incidence and second in mortality among cancers globally.¹ The gut microbiota is proximally located to the colorectal epithelium and continuously interacts with host cells. Recent evidence has shown that the gut microbiota plays an important role in CRC development² and greatly varies in CRC patients.³ Also, certain bacteria influence the efficacy of

cancer immunotherapy, this could be related to the activation of anti-tumor immune responses.^{4,5} Moreover, Tanoue et al isolated 11 bacterial strains from healthy donor feces. They found that a gavage of a mixture containing these 11 strains could inhibit the growth of subcutaneous tumors in mice and enhance the therapeutic effect of the anti-PD1 antibody.⁶

Bacterial toxins are important metabolites, which were used as a cancer treatment a 100 years ago, that often have powerful cytotoxicity and incite strong immune responses toward the host. In 1910, William Coley utilized *Streptococcus erysipelas* and *Bacillus prodigiosus* to successfully treat patients with inoperable sarcomas, these are known as Coley's toxins today. Among 52 cancer patients who received bacterial toxins treatment, 36 cases had partial responses or complete responses.⁷ The mechanisms by which these beneficial effects

CONTACT Jin Gu  zlguj@bjmu.edu.cn  Key Laboratory of Carcinogenesis and Translational Research, Ministry of Education, Peking University Cancer Hospital & Institute, Beijing 100142, China; Peking University Shougang Hospital, Beijing, China

*These authors contributed equally to this work.

 Supplemental data for this article can be accessed on the [publisher's website](#).

© 2020 The Author(s). Published with license by Taylor & Francis Group, LLC.

This is an Open Access article distributed under the terms of the Creative Commons Attribution-NonCommercial-NoDerivatives License (<http://creativecommons.org/licenses/by-nc-nd/4.0/>), which permits non-commercial re-use, distribution, and reproduction in any medium, provided the original work is properly cited, and is not altered, transformed, or built upon in any way.

occurred are partially due to the combination of the direct cytotoxic effect of the toxins and the activation of anti-tumor immune responses. With the development of biotechnology, a growing number of researchers are trying to use bacteria and their toxins to treat advanced cancers. In 1990, the live attenuated *Mycobacterium bovis* (Bacillus Calmette-Guérin, BCG) was approved as a treatment for bladder cancer.⁸ The best-known bacterial toxins with antitumor activity are anthrax toxin, *Pseudomonas aeruginosa* exotoxin A, and diphtheria toxin.^{9,10} By conjugating the toxin to antibodies or ligands, the engineered toxins could then selectively recognize cancer cells through surface antigens or receptors. These are known as immunotoxins and were much better tolerated by animals and have since been widely tested in human clinical trials.¹¹

Bacillus toyonensis (*B. toyonensis*), which is commonly found in the natural environment and gastrointestinal tract, is a nonpathogenic Gram-positive, rod-shaped, facultatively anaerobic, spore-forming bacterium. The bacterium was first identified as *Bacillus cereus* var *toyoi* but has recently been proposed as a new species named *B. toyonensis* because of its significant genomic differences from *Bacillus cereus*.¹² *B. toyonensis* has been widely used as a probiotic in animal feed for several decades.¹³ Some research has also suggested that *B. toyonensis* could exert an immunomodulatory function and enhance the response of traditional vaccines in mice and pigs.^{14,15} So far, there has been no report on its pathogenic nature. Abdulmawjood et al evaluated the enterotoxin gene expression of the *Bacillus toyonensis* BCT-7112 strain and found that the *hblC* gene was absent, therefore it was not able to form functional enterotoxins.¹⁶

Normal gut microbiota is a relatively unexplored treasure trove, which regulates many physiological processes, including nutrition metabolism, energy capture, and immune responses.^{17,18} However, the research about isolated bacteria as a cancer treatment is quite limited. In this study, we focused on the bacteria which were found to be universal in healthy individuals but generally absent in CRC patients in order to screen the strains and their metabolites for potential anti-tumor effects. A novel *Bacillus toyonensis* BV-17 was isolated from the feces samples of healthy donors, which

can secrete hemolysin BL (HBL) to quickly destroy the cell membranes of various tumor cells. To date, there have been no relevant reports about the anti-tumor potential of *B. toyonensis*. Here, we investigated the antitumor effects of HBL in vivo and in vitro in order to determine its potential as a cancer treatment for CRC.

Results

Genus Bacillus is common in healthy donors but absent in CRC patients

16S rRNA gene amplicon sequences were performed to analyze the gut microbiota characteristics between 25 CRC patients and 25 healthy donors (Table 1). In both groups, the *phylum Firmicutes*, *Bacteroidetes*, and *Proteobacteria* contributed to more than 96% of the total gut microbiota. However, the ratio between these bacteria significantly changed in the CRC patients. Among the CRC patients, the relative abundance of the *phylum Bacteroidetes* and *Proteobacteria* were significantly increased to 50.0 % and 10.3% (26.3% and 6.2 % in healthy donors), respectively, but the *phylum Firmicutes* was significantly decreased to 36.2 % (65.2% in health donors) (Figure 1(a)). Each sample data is shown in Supplementary Figure 1C. Similar results were obtained by LEfSe analysis (Supplementary Figure 1A-B), which were consistent with a previous study.¹⁹ After further analyzing the difference among the *phylum Firmicutes*, we found that despite the low abundance of the *genus Bacillus* in the gut, it was common in the healthy donors but absent in the CRC patients (Figure 1(b)). After this, all stool samples of the healthy donors were cultured to obtain these bacteria. However, only 4 of the 25 samples produced the typical colony morphology of the *genus*

Table 1. Characteristics of clinical samples and data.

	Healthy donors (n = 25)	CRC patients (n = 25)
Age (mean ± SEM)	50.60 ± 0.8981	61.64 ± 2.011
Male (no.,%)	64%	68%
Observed species per samples ^a	625.3 ± 19.45	749.6 ± 28.18
Stage I		7
Stage II		8
Stage III		8
Stage IV		2

^aSignificant difference of $P < 0.05$, using unpaired t test.

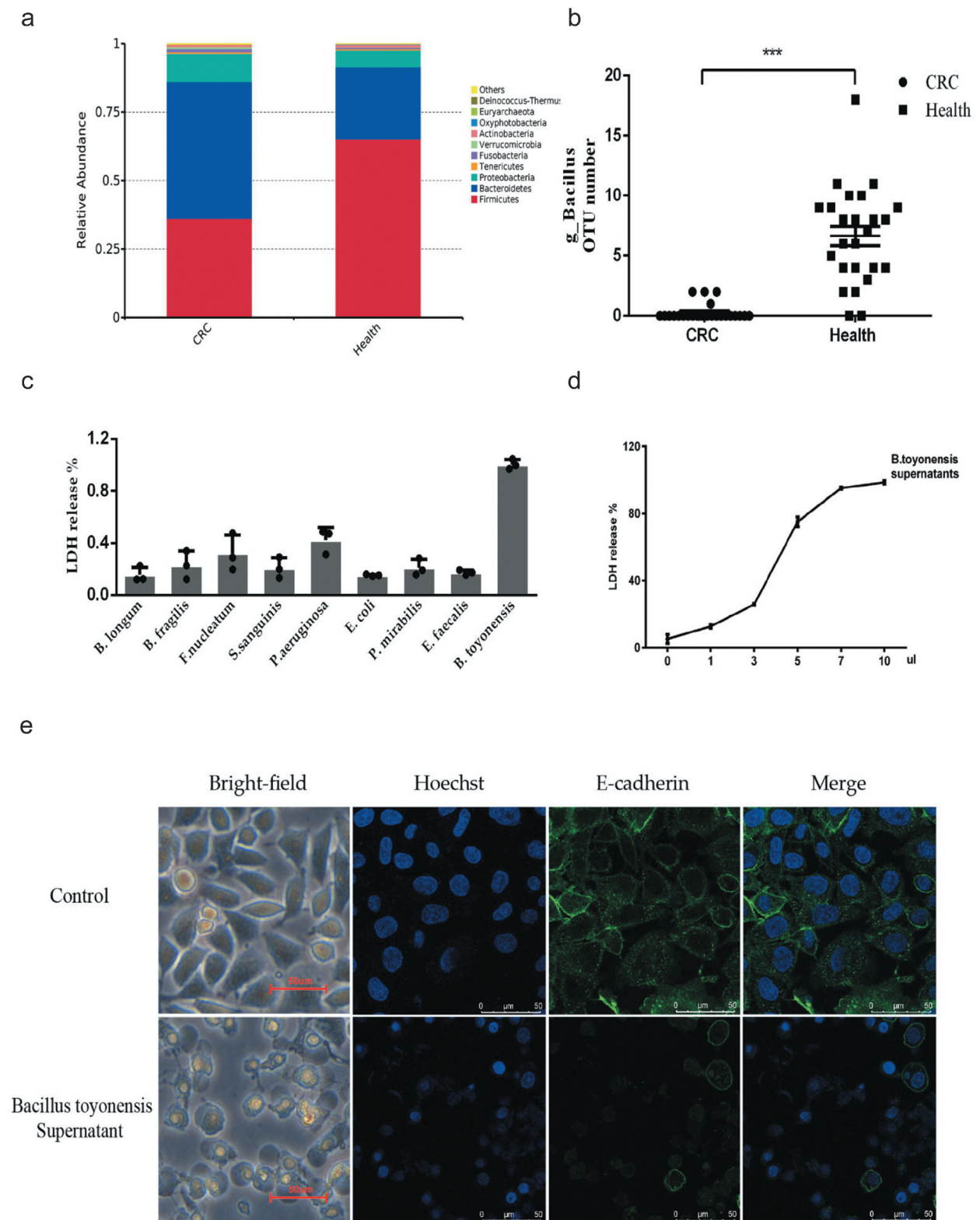


Figure 1. The secretion of *Bacillus toyonensis* BV-17 quickly kills tumor cells. (a) The top 10 relative abundance at the phylum level in the two groups. (b) The scatter plot of *genus Bacillus* OTU numbers in the two groups (** $p < .001$, unpaired student's t test, data were from the mean with SEM). (c) LDH release assay is used to measure the cell lysis of supernatants from different bacteria. Data are from the mean with SD in triplicates. (d) The cell lysis of *B. toyonensis* BV-17 supernatants is dose-dependent. The different volumes of supernatant (0 μ l to 10 μ l) are added to the 100 μ l cell culture medium incubating for 30 min. Data are from the mean with SD in triplicates. (e) The membrane damage of cells is shown by an indirect immunofluorescent assay.

Bacillus, this may be due to its low relative abundance. The colonies of these bacteria are round, milky, opaque, dry, and slightly convex when grown on blood agar and lecithinase positive on egg yolk agar. The bacterium is gram-positive, motile, and rod-shaped (Supplementary Figure 2A-C).

The secretion of *B. toyonensis* BV-17 quickly kills tumor cells by damaging the plasma membrane

By co-culturing HCT8 tumor cells with secretions from the different isolated bacteria of the stool samples, we found that only the supernatants from the isolated bacteria of the genus *Bacillus* led to total cell lysis in a short period (Figure 1(c)). This result greatly varied among the different clones of these bacteria. As such, we focused on the clone with the most powerful cytotoxicity for species identification. Using 16S rRNA gene sequencing, the species was revealed to most likely be *Bacillus toyonensis* BCT-7112 (Supplementary Figure 2E). However, there is a high similarity between the 16S rRNA gene sequences between *Bacillus* groups, therefore we conducted whole-genome sequencing. The results, once again, identified the species to most likely be *B. toyonensis*, with 99.651% identity and 89.8% coverage to the type genome of *B. toyonensis*. This strain was named *B. toyonensis* BV-17 and uploaded to NCBI (accession number: CP047044) (Supplementary Figure 2D)

Lactate dehydrogenase (LDH) is a stable cytosolic enzyme that is released upon cell lysis. Almost all the cells died after the addition of 10 μ l supernatant to a 100 μ l cell culture in 30 min (Figure 1(d)). At first, balloon-like shapes emerged around the cell, and then the cell membranes broke. To prove cell death, we marked the cell membranes with an anti-E-cadherin antibody, which is a membrane protein, and marked the cell nucleus with Hoechst. Compared to the control group, the cell membranes were destroyed and the nuclei shrank in the *B. toyonensis* BV-17 supernatant group. (Figure 1(e)).

Characteristics of the effector in the supernatant of the *B. toyonensis* BV-17 culture

To analyze the biological characteristics of the unknown active agent, we incubated cells with the

supernatant of *B. toyonensis* BV-17 cultures treated to 50°C heat, 75°C heat and proteinase K for 1 h. The supernatant from cultures treated with 75°C heat or proteinase K no longer produced the cytotoxicity effect. However, the supernatant treated with 50°C heat still retained this effect (Supplementary Figure 3A). Size-fractionation of the supernatants using different ultrafiltration tubes revealed that the >10 kd and >30 kd fractions included the effector protein (Supplementary Figure 3B). Collectively, it was determined that the effector is a heat-sensitive protein with a molecular weight of more than 30 kDa.

To identify the effector protein, the supernatants were purified using Superdex 200 10/300 GL gel filtration columns with fast protein liquid chromatography (FPLC). Every eluted fraction was tested for the degree of cell bleb emergence and cell membrane disruption. Of the 67 eluted fractions (Figure 2(a)), only the 23rd, 24th, and 25th fractions had powerful cytotoxic activity against tumor cells (Figure 2(b)). These positive fractions were collected and analyzed with 12% SDS-PAGE (Figure 2(c)). The mass spectroscopy analysis revealed hemolysin BL lytic component L2 (HBL-L2), hemolysin BL lytic component L1 (HBL-L1) and hemolysin BL binding component (HBL-B). These proteins belong to a homologous three-component enterotoxin (Table 2). When expressing and purifying these three proteins in the *E. coli* BL21 (Figure 2(d)), the results showed that any single component or HBL-L2 combined with HBL-B produced no cytotoxicity. However, when combining HBL-L1 with HBL-L2 or HBL-B, the cells were quickly killed (Figure 2(e)). Moreover, this cytotoxicity had no strict sequential manner as no matter which component was added to the cell first, cell lysis occurred as long as one of the two protein components was HBL-L1 (Figure 2(f)).

HBL secreted from *B. toyonensis* BV-17 rapidly kills cancer cells in high concentrations and significantly inhibits cell proliferation in low concentrations

To obtain the reaction time of HBL, we tested the time to cell death by adding high doses of HBL (10 μ g/ml) to cancer cell cultures. With increasing HBL concentrations in the cell cultures, the time till cell death was significantly shortened. Cancer cells

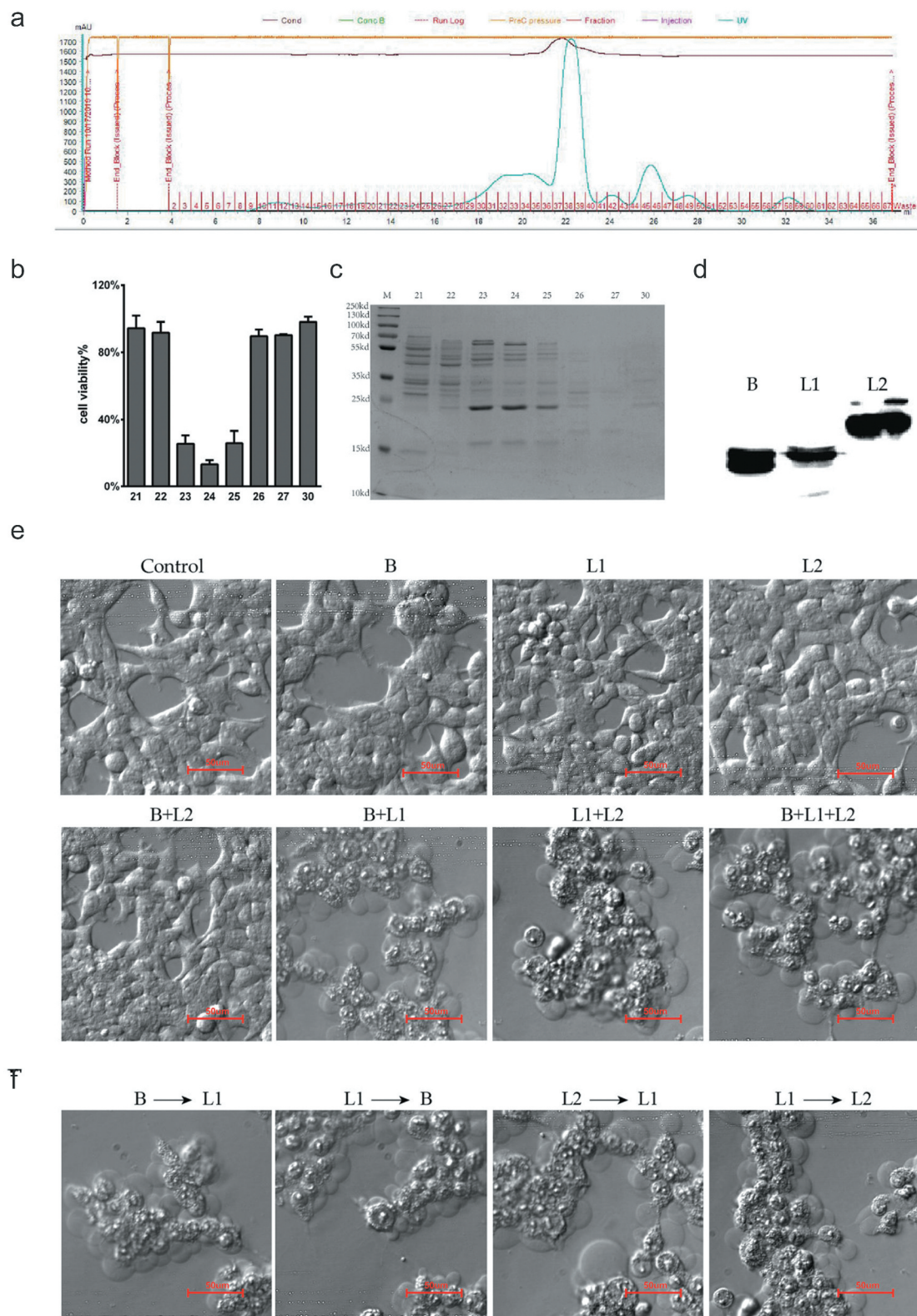


Figure 2. Identification of the effectors in the supernatants of *B. toyonensis* BV-17. (a) FPLC chromatogram of the secretion from *B. toyonensis* BV-17. The horizontal axis shows the eluted fractions (67 in total). The blue curve shows the absorbance at A280. (b) Cell viability by CCK-8 assay is conducted after exposure to different eluted fractions. Data are from the mean with SD in triplicates. (c) 12% SDS-PAGE gel analysis of eluted proteins with coomassie staining. M: marker. 23–25 (cytotoxic fractions). 21, 22, 26, 27, 30 (adjacent non-cytotoxic fractions). (d) Expression analysis of the recombinant HBL-B, HBL-L1, and HBL-L2 in the *E. coli* BL21 by Western blotting. (e) Mechanism of cytotoxicity toward the HCT116 cells among three components of HBL. The cells are treated with 10 µg/ml recombinant proteins for 5 min. (f) Sequential action manner analysis of the HBL three components.

Table 2. Main toxins in the 23rd, 24th, and 25th fractions by mass spectroscopy analysis.

Description	Accession	Coverage [%]	MW [kd]	Score
Hemolysin BL component L2 OS = <i>Bacillus cereus</i>	R8U655	72	49.3	608.46
Hemolysin BL component L1 OS = <i>Bacillus cereus</i>	C2PF09	18	43.9	11.5
Hemolysin BL component B OS = <i>Bacillus cereus</i>	P80172	54	41.5	1622.08

began bubbling in just 5 min and were almost totally dead in 10 min (Figure 3(a)). By detecting Annexin V/PI-double positive cells with flow cytometry, we found that the cell death rate reached almost 50% in just 5 min (Figure 3(b,d)). Further investigations revealed that HBL exhibited similar cytotoxicity on HCT116, HeLa, B16-F10, and A549 cancer cell lines, which originated from colorectal cancer, cervical cancer, melanoma, and lung cancer, respectively. Unfortunately, HBL also killed the IEC6 cell cultures, a normal rat intestinal epithelial cell line (Figure 3(c)). Thus, the toxin not only kills cancer cells but also normal mammalian cells. We determined that the cytotoxicity of HBL is dose-dependent by using the CCK-8 assay. The half-maximal inhibitory concentration (IC 50) of HBL is quite low, about 0.5 $\mu\text{g/ml}$ (Table 3). When cancer cells were incubated with low doses of HBL, such as 0.1 $\mu\text{g/ml}$ and 0.25 $\mu\text{g/ml}$, obvious cell lysis and bleb were not induced, but over time the cancer cell proliferation and clone formation were significantly inhibited. When the concentration was increased to 0.5 $\mu\text{g/ml}$, all the cells died and no clones formed (Figure 3(e-g)).

HBL inhibits the growth of both treated and untreated tumors in vivo

To preliminarily evaluate the antitumor effects of HBL in vivo, we established a colorectal subcutaneous tumor model. Firstly, the MC38 tumor model was used to test HBL treatment on small tumors in C57BL/6 mice, which have an intact immune system. To reduce nonspecific cytotoxicity, we treated the tumors with intra-tumor injections containing 10 μg HBL in just 25 μl . The control group consisted of tumor-bearing mice treated with intra-tumor injections of 25 μl PBS buffer. The results showed that tumor growth in the HBL group was significantly inhibited. (Figure 4(a-c)).

Interestingly, the spleen volume was also increased in the HBL group, which could be related to the activation of immune responses (Figure 4(d-e)). Secondly, the human HCT116 tumor model was used to test the treatment of large tumors in nude mice, which are genetically mutated to have a deficient immune system. When the tumor volume reached roughly 250 mm^3 by day 13, localized HBL treatment was administered every 3 days to the mice. After which, we found similar results to the C57BL/6 mice experiments. Tumor volume in the HBL group was significantly smaller than the control group and even shrank when compared with before treatment volumes (figure 4(f-h)). To test the toxicity of HBL, we monitored the changes in body weight and normal tissue damage in nude mice. Apparent physical discomfort and weight loss were not found when using the localized treatment (Supplementary Figure 4A-B), but localized necrosis occurred 1 day after the injection. However, unlike a classic inflammatory response, there was no obvious redness or swelling at the injection site (Supplementary Figure 4C-D). To detect whether the treatment had a distal effect, we successfully established a bilateral subcutaneous MC38 tumor model. The right-side tumor was treated with intra-tumor injections of HBL (5 μg HBL in 25 μl) or PBS every 3 days, while the left-side tumor remained untreated (Figure 5(a)). For the treated tumor, the growth rate of subcutaneous tumors was significantly slower than the control group. The treatment resulted in tumor tissue completely disappearing from 2 mice, with increasing treatment times and doses (Figure 5(b-c)). For the untreated tumor, HBL delayed tumor growth to some extent (Figure 5(d-e)).

Infiltrating T lymphocyte increases in both treated and untreated tumors of the HBL group

We found that there were necrotic and inflammatory cells infiltrating the HBL treated tumors by hematoxylin-eosin (H&E) and immunohistochemical (IHC) staining. As for the untreated tumors of the HBL group, although no necrosis was found, tumor-infiltrating T cells were significantly increased (Figure 6(c-f)). Moreover, no obvious differences or necrosis were found in distant organs (heart, liver, spleen, lung and kidney) between the HBL and control groups (Figure 6(a,b)).

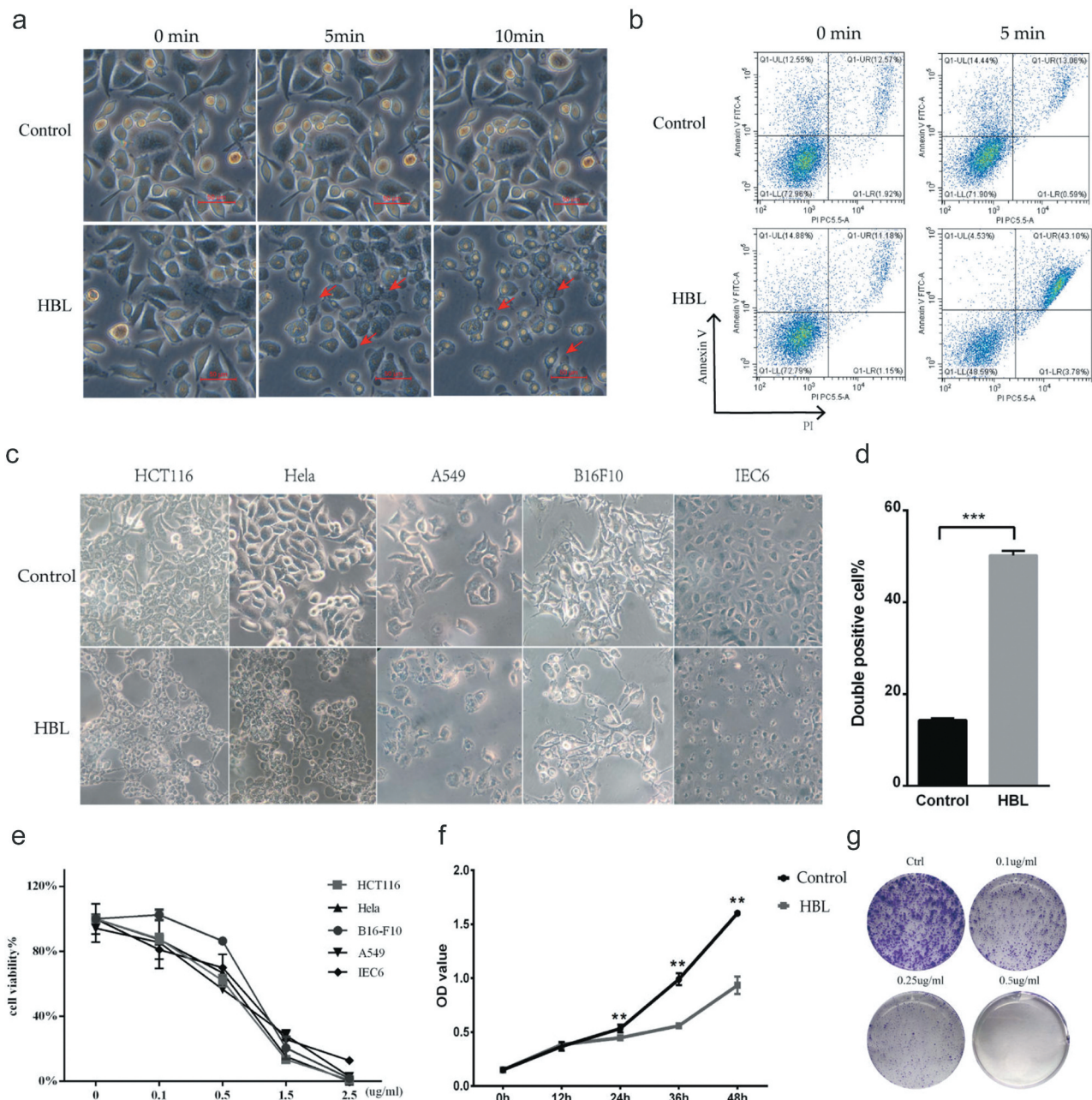


Figure 3. HBL rapidly kills various cancer cells with high concentrations and significantly inhibits cell proliferation with low concentrations. (a) The morphology changes of cells in treatment with 10 µg/ml HBL over time. Red arrows represent the dead cells with blebs formation. (b) Apoptosis analysis by flow cytometry after incubating with HBL for 5 min. (c) The alterations of various cell morphology after exposed to 2.5 µg/ml HBL toxins for 30 min. (d) Histogram of double-positive cells in HBL and control groups, which represent the dead cells. (e) Cell viability by CCK-8 assay is conducted after exposure to different concentrations of HBL toxins. (f) Cell proliferation is measured by CCK-8 assay within 48 hours. HCT116 cancer cells are treated with HBL at 0.1 µg/ml and PBS, respectively. (g) Clone formation assay of HCT116 cancer cells treated with different concentrations of HBL. (*** $p < .001$, ** $p < .01$, unpaired student's t test, data are from the mean with SD in triplicates).

Discussion

In this study, we found that the *genus Bacillus* is common in healthy donors but absent in CRC patients. According to previous studies, various strains of *genus Bacillus*, such as *Bacillus subtilis*,

Bacillus licheniformis, *Bacillus cereus*, and *Bacillus toyonensis*, are widely used as probiotics in animal feed and have also been used in the treatment of diarrhea, intestinal dysfunction, and enteritis in humans.^{20–22} In addition to the HBL secreted by

Table 3. Cytotoxic activity of HBL toxins against various mammal cells.

Cell name	Characteristics	IC50(μ g/ml)
HCT116	Colorectal cancer	0.48
Hela	Cervical cancer	0.52
B16-F10	Melanoma	0.80
A549	Lung cancer	0.52
IEC-6	Normal intestinal cell	0.67

B. toyonensis BV-17 being able to rapidly kill cells in vitro, the mice treated by oral gavage with 1×10^8 cfu live bacteria or even a 25-fold concentration of the bacterial supernatants did not show any discomfort. We suspect that an intact intestinal mucosal barrier may help to protect against the toxicity of HBL. When developing colorectal cancer, tumor tissues are often accompanied by bleeding and destruction of the mucosal barrier. In this case, the HBL produced by *B. toyonensis* BV-17 may kill tumor cells and incite an immune response that slows the progress of the tumors. However, further research is required to test this hypothesis in vivo.

HBL is a three-component enterotoxin secreted from *Bacillus cereus* and an intact protein has not been found in *Bacillus toyonensis* until now. Kovac et al²³ evaluated the production of HBL proteins (L1, L2, and B) among the *Bacillus* species from the perspective of phylogeny. They performed whole genome sequencing of 22 *Bacillus* species isolated from dairy and found that HBL was neither inclusive nor exclusive to *B. cereus*, which varies a lot. Many strains of genus *Bacillus* contain homologs of the *hblACD* gene but do not produce HBL, possibly due to amino acid substitutions in the different toxin-encoding genes. As for the mechanism of action, the component B (41.5 kDa) binds to the cell surface and then the two lytic determinant components L1 (43.9 kDa) and L2 (49.3 kDa) form pores in the cell membrane.²⁴ Moreover, neither any single component nor any combination of two components showed cytotoxicity. This tripartite toxin is aggregated in a strictly sequential manner (B-L1-L2) and the binding component B is crucial to its toxicity.²⁵ In contrast, by expressing the three HBL proteins from *B. toyonensis* BV-17 in *E. coli* BL21, we found that its mechanism of action differed from the previous studies described above. Combining two components (L1 + B or L1+ L2),

provided one of the components is L1, exhibited a powerful toxicity toward cells and did not adhere to a sequential manner. The HBL-L1 is essential for the cytotoxicity, and only one of the other HBL-B or HBL-L2 is needed to kill cells. We analyzed multiple sequence alignments of the recombinant HBL and determined it has high homology with previous research (B: 95.4% identity, L1: 99.8% identity, L2: 97.9% identity). With the main difference being that the HBL-L1 simply replaces A with V at the 45th amino acid position (Supplementary Figure 5A-C).

Mathur et al²⁶ found that HBL could induce pyroptosis in bone marrow-derived macrophages (BMDMs) accompanied by the secretion of IL-1 β and IL-18 which incites inflammation in mice. Another study showed that pyroptosis of tumor cells can induce inflammation and then trigger robust anti-tumor immune responses.²⁷ Gil M et al²⁸ demonstrated that IL-18 is positively correlated with CD8(+) T Cell and natural killer cell infiltration in skin cutaneous melanoma. We also speculate that cytoplasmic proteins leaked from cancer cells may contribute to the activation of the immune system due to exposure of tumor neoantigens. Our results demonstrated that HBL inhibited the growth of not only treated tumors but also untreated tumors in mice, exhibiting increased tumor-infiltrating T cells in both tumor types. However, nonspecific cytotoxicity limits the application of HBL treatment as this characteristic determines that it is not suitable for systemic administration. Even so, HBL is a modifiable protein. One solution is to conjugate the toxin to a tumor-specific antibody or ligand to create a immunotoxin, which can selectively recognize antigens or receptors on the cancer cell surface. This approach has proven feasible in solving the tumor-targeting problem for other toxins, such as anthrax toxin, *Pseudomonas aeruginosa* exotoxin A, and diphtheria toxin.¹⁰ Moreover, HBL has its added advantages compared to existing toxins for cancer therapy: 1. HBL kills cells not by entering the cell but by acting on the plasma membranes, which allows it to continue to function efficiently after re-engineering, 2. Each single component of HBL shows no cytotoxicity, which enables its exogenous expression in *E. coli* without causing host cell death

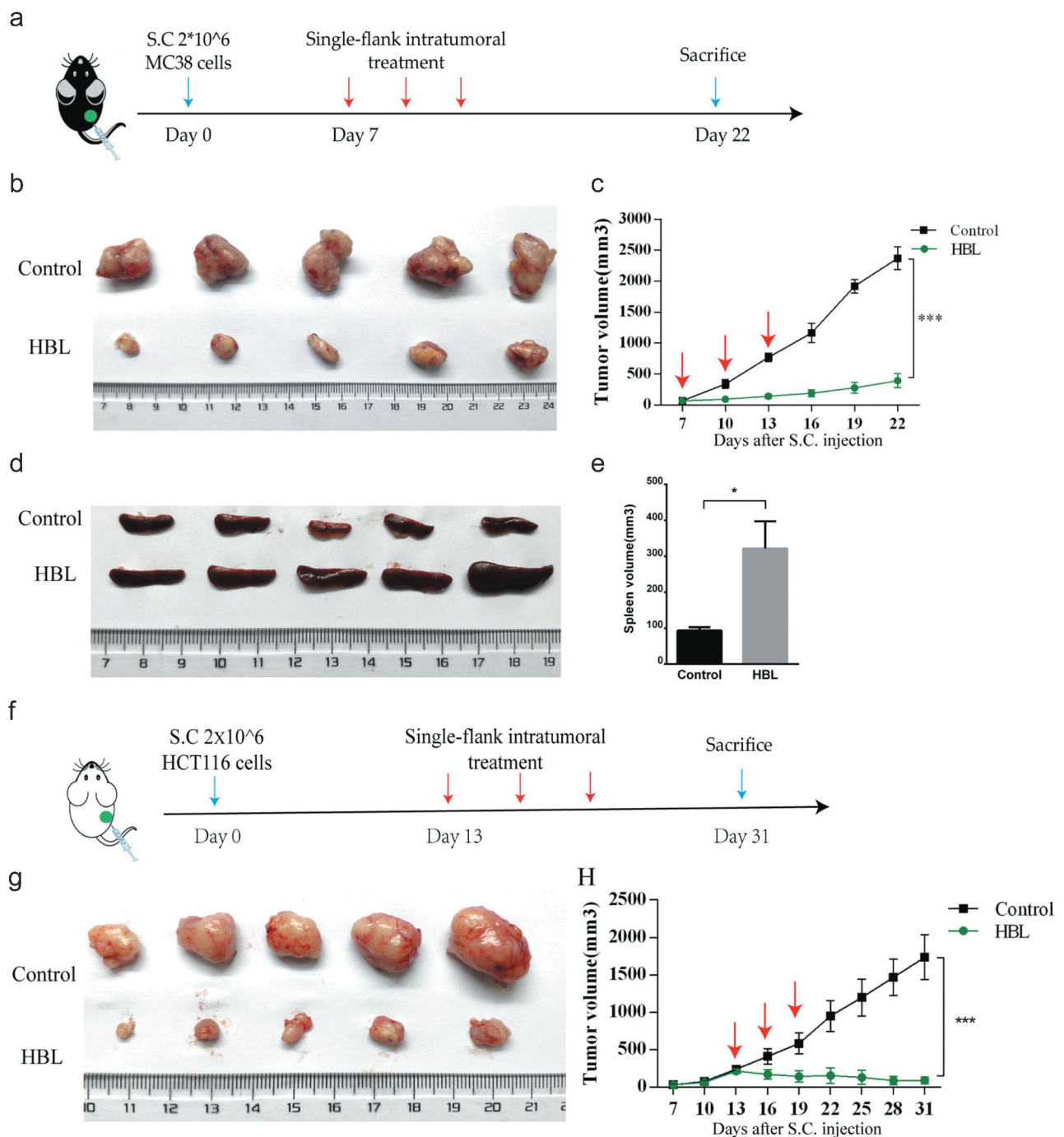


Figure 4. HBL significantly inhibits the growth of subcutaneous tumors in vivo. (a) The schedule of experiments in C57BL/6 mice. (b) The excised tumor tissues of C57BL/6 mice from the two groups at day 22. (c) Measurement of MC38 tumor volume in the two groups over different day points. (d) Gross morphology of the spleen from the two groups in sacrificed mice. (e) Histogram of the spleen volume in the two groups. (f) The schedule of experiments in nude mice. (g) The excised tumor tissues of nude mice from the two groups at day 31. (h) Measurement of HCT116 tumor volume in the two groups over time. (***) $p < .001$, (*) $p < .05$, unpaired student's t test, data are from the mean with SEM. Red arrows represent one treatment).

facilitating mass production, 3. The two components working together to produce cytotoxicity can be used to improve treatment safety. In summary,

HBL has antitumor activity and is a potential chemotherapeutic agent that, in future, could be re-engineered to specifically target tumor cells.

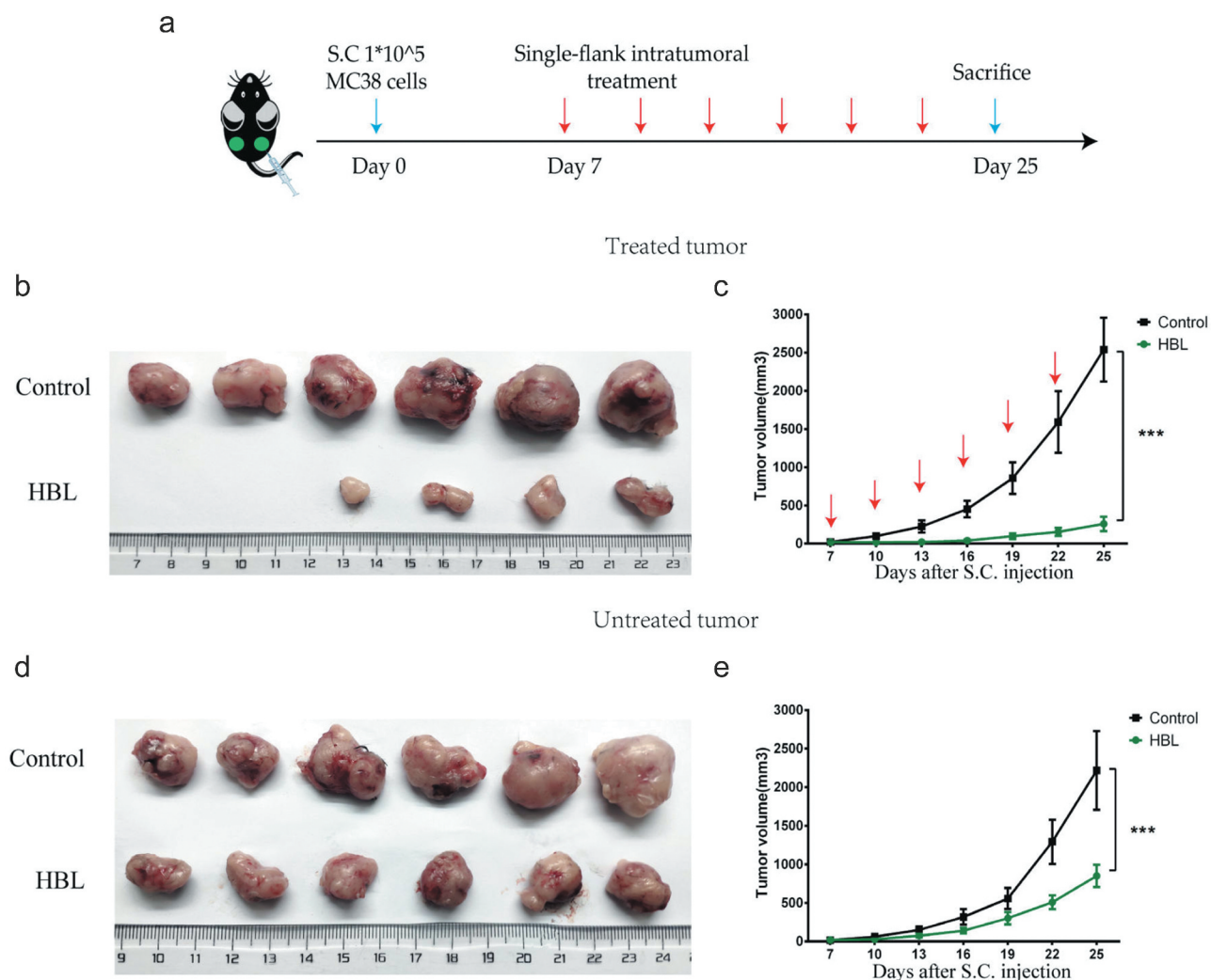


Figure 5. HBL also inhibits the growth of untreated tumors in vivo. (a) The schedule of experiments in vivo. 1×10^5 MC38 cells were subcutaneously injected into the bilateral sub-axillary tissues. (b) The excised treated tumor tissues of C57BL/6 mice from the two groups at day 25. (c) Measurement of treated MC38 tumor volume in the two groups over time. (d) The excised untreated tumor tissues of C57BL/6 mice from the two groups at day 25. (e) Measurement of untreated MC38 tumor volume in the two groups over time. (***) $p < .001$, unpaired student's t test, data are from the mean with SEM. Red arrows represent the treatment.).

Materials and methods

Patient feces collection and 16S rRNA gene sequencing

The collection of all samples and information was approved by the Ethics Committee of Peking University Shougang Hospital. All patients provided verbal consent for this study. From September 2017 to September 2018, a total of 50 people were enrolled in this study, including 25 healthy donors from the department of physical examination and 25 patients with colorectal cancers from the department of gastrointestinal surgery. None of the CRC patients had undergone radio-chemotherapy at the time of

enrollment. No participants had undergone any antibiotic treatments three months prior to enrollment. Fecal samples from the CRC patients and healthy volunteers were collected and stored at -80°C . The genomic DNA, library construction, and 16S rRNA sequencing were performed by Novogene Company.

Bacteria isolation and identification

Feces (0.5 g) from the healthy donors were homogenized in 5 ml of sterile PBS in a 15 ml sterile centrifuge tube. Centrifugation was carried out at 1000 RPM for 1 min and then a 50 μl

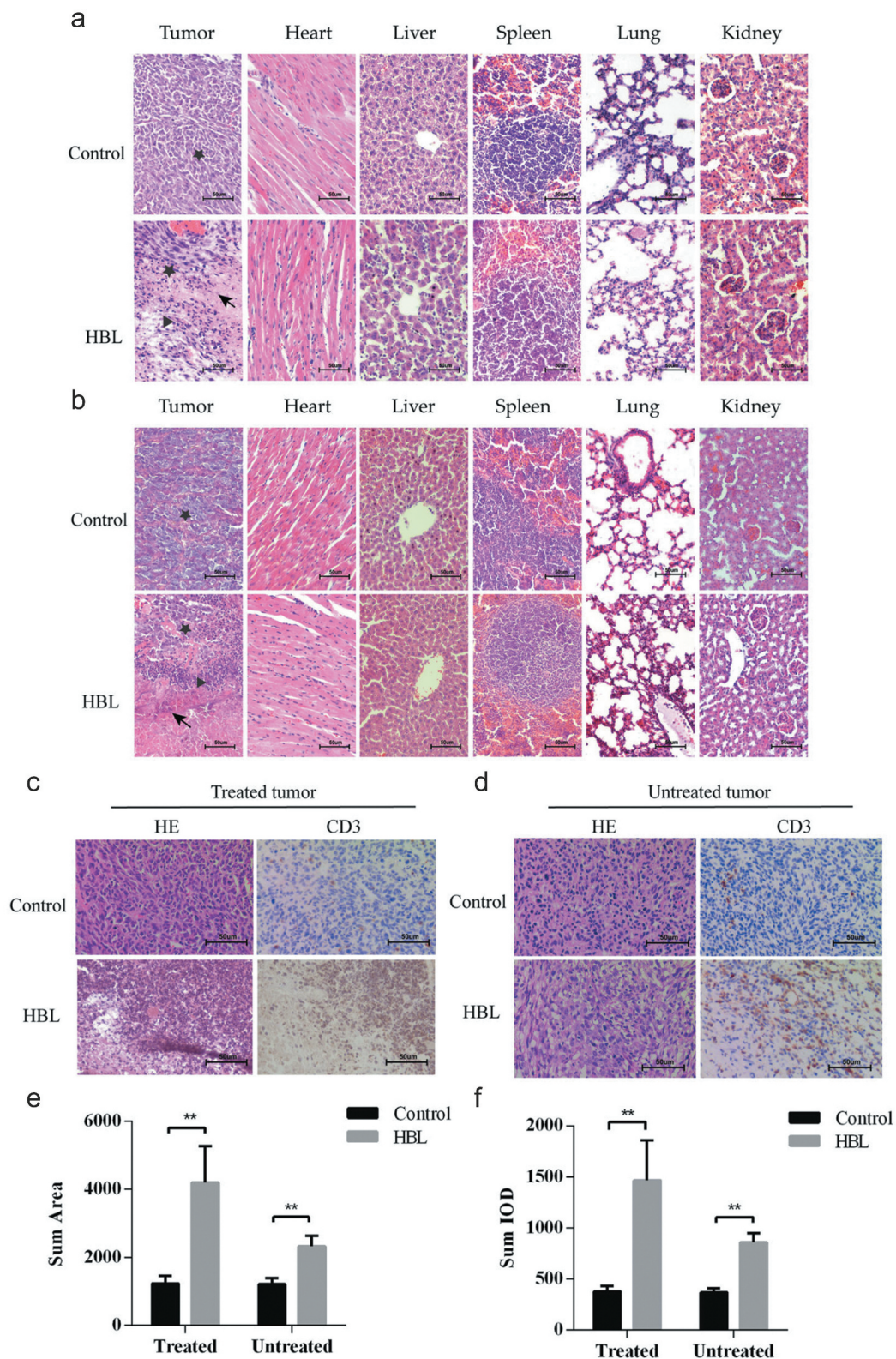


Figure 6. Histological evaluation of tumor tissues and distant organs. (a) The effect of HBL treatment on MC38 tumor tissues and distant organs in C57BL/6 mice. (b) The effect of HBL treatment on HCT116 tumor tissues and distant organs in nude mice. (c) The histological change and T cell infiltration in treated MC38 tumor tissues of the HBL group. (d) The histological change and T cell infiltration in untreated MC38 tumor tissues of the HBL group. (e) Histogram of sum area in T cell infiltration on both sides of MC38 tumor. (f) Histogram of sum IOD (integral optical density) in T cell infiltration on both sides of MC38 tumor. (★ represents tumor cell, ▲ represents inflammatory cells, and ↘ represents necrosis, ** $p < .01$, unpaired student's t test, data are from the mean with SEM. Red arrows represent the treatment.).

aliquot of the supernatant was directly spread onto blood agar plates. The plates were incubated at 37°C for up to 3 days under both anaerobic and aerobic conditions. After which, a sterile inoculation needle was used to pick up single colonies and streak them on clean plates in order to culture pure colonies. Pure colonies of interest were examined by Gram-stain under a light microscope and by PCR for colony identification. Briefly, pure colonies were inoculated into a 100 µl Eppendorf tube containing 50 µl sterile water, this bacterial suspension was then boiled for 20 min at 99°C and cooled to 4°C. The resulting DNA (2 µl) was used in a 50 µl PCR reaction with universal bacterial primers, 27F (AGAGTTTGATCCTGGCTCAG) and 1492R (TACGGCTACCTTGTACGACTT) to amplify the bacterial 16S rRNA gene. The PCR products were sequenced by TIANYI HUIYUAN Company and blasted on the NCBI database to preliminarily identify the isolated bacteria. As for whole-genome sequencing, the bacterial genomic DNA was extracted using a TIANamp Bacteria DNA Kit (DP302), according to the manufacturer's instructions, and then sequenced with Illumina PE150 by Novogene Company.

Cell cultures and animals

The mammalian cell lines including HCT8, HCT116, MC38, HeLa, B16-F10, A549, and IEC-6 were purchased from the National Infrastructure of Cell Line Resource in Beijing. They were routinely tested and authenticated using a panel of genetic and epigenetic markers. Cells were cultured in DMEM or RPMI-1640 medium with 10% FBS at 37°C in a humidified incubator (5% CO₂) and passaged in our laboratory for 1 month after resuscitation. The 6–8 weeks old female C57BL/6 mice and Nude mice were purchased from Vitalriver Experimental Animal Technology Co. Ltd. (Beijing, China) and raised in an SPF (specific pathogen-free) environment. All animal experiments were conducted in accordance with the guidelines of the Animal Welfare and Research Ethics Committee of Peking University Cancer Hospital (Permit Number: EAEC 2018–20).

LDH releasing assay

Lactate dehydrogenase activity released in the culture media was measured by the CytoTox 96® Non-Radioactive Cytotoxicity Assay (Promega), according to the manufacturer's instructions. The absorbance at 490 nm was recorded using a microplate reader. LDH release % = (Experimental LDH Release (OD490)/Maximum LDH Release (OD490)) x 100.

Cell indirect immunofluorescent assay

1×10^6 HCT8 cells were seeded in a confocal dish and cultured overnight. The *B. toyonensis* BV-17 supernatants (100 µl) were added to the 1 ml of cell culture media in the confocal dish. When cell blebs emerged and destruction of the cell membrane had occurred, the culture media was removed and the cells were fixed with 4% paraformaldehyde for 5 min. To permeabilize the cell membranes, the cells were treated with 0.5% Triton x100 for 20 min. Then blocked with goat serum for 1 h. After which, the cells were stained with a rabbit monoclonal antibody against E-cadherin (ab15148, Abcam) at 4°C overnight. Following this, the cells were stained with the secondary antibody conjugated with Alexa Fluor® 488 (Goat anti-rabbit IgG, ab150077, Abcam) at room temperature for 2 h. The cell nucleus was stained with Hoechst33342 for 5 min. The results were observed with a laser confocal microscopy.

Isolation of effective proteins from *B. toyonensis* BV-17 supernatants by FPLC and identification by mass spectrometry

B. toyonensis BV-17 was seeded into 500 ml LB medium and grown at 37°C for 36 h. The supernatant was then concentrated into 1 ml with a 10 kd ultrafiltration tube (Millipore). The upper liquids were collected and purified by Superdex 200 10/300 GL gel filtration columns with FPLC. A total of 36 ml of elution buffer was flowed at the rate of 0.5 ml/min and 0.5 ml was collected in 1.5 ml Eppendorf tube. The component and molecular mass of eluted proteins were analyzed by 12% SDS-PAGE. The SDS-PAGE gel was stained with Coomassie Brilliant Blue Staining Solution. After which, the gel containing the proteins was cut and

digested with trypsin. The digested peptides were then identified by MALDI-TOF mass spectrometry.

Expression, purification, and western blotting analysis of the recombinant HBL (rHBL)

The *hblC* (L2), *hblD* (L1), *hblA* (B) genes were amplified from the *B. toyonensis* BV-17 genome by PCR. The primer pairs were: HBL-B-F-BamH1: CGCGGATCCATGATGAAAAATATCCCGTACAACT, HBL-B-R-Hind3: CCCAAGCTTTTTTTTGTGGAGTAACAGTTTCCAC, HBL-L1-F-BamH1: CGC GGATCCATGATGAAAAAATCCCA TTCAAAGTG, HBL-L1-R-Hind3: CCC AAGCT TTTCTGTTTAAAAGCGATGTCTTT, HBL-L2-F-BamH1: CGC GGATCCATGAAGAATAAAA TAATGACAGGATTTTTAATAACAT, and HBL-L2-R-Hind3: CCCAAGCTTAAATTTATATACC TGTTCTTCAAGGTAAGTACTTATT. Then the sequences were cloned into the pET-28a vector, which added an N-terminal and C-terminal 6xHis-tag to the protein. The rHBL was expressed in *E. coli* BL21 chemically competent cells induced by 0.1 mM IPTG (isopropyl-1-thio- β -D-galactopyranoside) for 6 h at 37°C. The protein was purified using a Ni-NTA resin column and analyzed by western blotting with the primary Rabbit anti-6xHis tag antibody (Abcam: ab9108).

Cytotoxicity and apoptosis assays

Cytotoxicity was measured with a CCK-8 assay. In brief, 2×10^4 various mammalian cells were seeded in 96-well plates and grown overnight in 100 μ l culture medium. Then the cells were incubated with different concentrations of toxins at 37°C for 30 min. Each dose gradient had 3 duplications. After which, 10 μ l of CCK-8 solution as added to each well and incubated for 1 h. The absorbance at 450 nm was recorded by microplate reader. Cell viability % = $[A(\text{HBL}) - A(\text{blank})] / [A(\text{control}) - A(\text{blank})] \times 100\%$. Apoptosis was measured with an Annexin V-FITC Apoptosis Detection Kit (Beyotime), according to the manufacturer's instructions. In brief, 1×10^6 HCT8 cells were seeded in a 12-well plate and grown overnight. The cells were then treated with 10 μ g/ml HBL or PBS. After 5 min, the cells were stained with 5 μ l Annexin V-FITC and 10 μ l PI for 20 min at room temperature. Then the cells were detected by flow cytometry.

Cell proliferation and clone formation assays

Cell proliferation was measured by CCK-8 assay. In brief, 1×10^4 HCT116 cells were seeded in 96-well plates and grew overnight with 100 μ l culture medium. Then the cells were incubated with 0.1 μ g/ml HBL or equal PBS at 37°C. The cell counts were positively correlated with OD value and measured every 12 hours with five-time points. Each time point had three duplications. For clone formation assays, 1×10^3 HCT116 cells were seeded into a 6-well plate and grew overnight. Then the cells were treated with 0.1 μ g/ml, 0.25 μ g/ml, 0.5 μ g/ml and equal PBS respectively. After growing at 37°C in 5% CO₂ for 2 weeks, the cells were fixed with 4% paraformaldehyde for 15 min and then the cell colony was stained with crystal violet dye and the colony-forming efficiency in the different groups was determined.

Animal experiments

The C57BL/6 mice or nude mice were used to establish tumor models and randomly divided into two groups. For the one-side tumor model, 2×10^6 MC38 or HCT116 cells in 100 μ l serum-free RPMI-1640 medium were subcutaneously injected into the right sub-axillary tissues. When tumor volume reached about 100 mm³ at day 7 or 250 mm³ at day 13, C57BL/6 or nude mice began to receive the intra-tumor injection of HBL (10 μ g HBL in 25 μ l) or PBS every 3 days, receiving a total of 3 treatments. For the two-side tumor model, 1×10^5 MC38 cells in 100 μ l serum-free RPMI-1640 medium were subcutaneously injected into the bilateral sub-axillary tissues. When tumor volume reached about 50 mm³ at day 7, the right-side tumor was treated with an intra-tumor injection of HBL (5 μ g HBL in 25 μ l) or PBS every 3 days, while the left-side tumor remained untreated. All mice were sacrificed when tumor volumes reached about 2000 mm³. Tumor volume and the weight of the mice were measured every 3 days. Tissue volume was calculated by the formula: Volume = (Length x Width²)/2. Tumors and other organs were removed and fixed with 4% paraformaldehyde for further research. The protein concentration was measured with a BCA assay.

Histological evaluation

Tumors and other organs were removed from the mice and washed with PBS. All tissues were fixed with 4% paraformaldehyde overnight, then dehydrated by graded ethanol, vitrified by dimethyl benzene and finally embedded in paraffin. Serial 5.0 μm tissue biopsies were cut and used for H&E staining and IHC staining. The T cell infiltration in the tumors were marked by anti-CD3 antibodies (ab16669, Abcam). Image-pro Plus software was used to quantitatively calculate the sum area and sum IOD of the CD3 staining in tumor tissues. The necrosis and inflammation were compared between the two groups in a blind manner.

Statistical analysis

The data of cell experiments were carried out in triplicates and the data of animal experiments was independently repeated twice. The results were shown as mean with SD or with SEM. The results were considered statistically significant if the *p*-value was less than 0.05. The graphs and the statistical analysis were conducted by Graphpad Prism version 6.0.

Acknowledgments

We would like to thank Professor Xing Chen at the College of Chemistry and Molecular Engineering, Peking University for his support in protein purification by FPLC.

Disclosure of Potential Conflicts of Interest

The authors declare no conflict of interest.

Funding

This work was supported by Beijing Natural Science Foundation [grant no. Z171100001017087] and Ministry of science and technology [grant no. 2016YFC1302605].

ORCID

Jiajia Chen  <http://orcid.org/0000-0002-5363-1389>
Zhaoya Gao  <http://orcid.org/0000-0002-0874-2266>

References

1. Bray F, Ferlay J, Soerjomataram I, Siegel RL, Torre LA, Jemal A. Global cancer statistics 2018: GLOBOCAN estimates of incidence and mortality worldwide for 36 cancers in 185 countries. *CA Cancer J Clin.* 2018;68(6):394–424. doi:10.3322/caac.21492.
2. Wong SH, Zhao L, Zhang X, Nakatsu G, Han J, Xu W, Xiao X, Kwong TNY, Tsoi H, Wu WKK, et al. Gavage of fecal samples from patients with colorectal cancer promotes intestinal carcinogenesis in germ-free and conventional mice. *Gastroenterology.* 2017;153(6):1621–1633 e6. doi:10.1053/j.gastro.2017.08.022.
3. Yu J, Feng Q, Wong SH, Zhang D, Liang QY, Qin Y, Tang L, Zhao H, Stenvang J, Li Y, et al. Metagenomic analysis of faecal microbiome as a tool towards targeted non-invasive biomarkers for colorectal cancer. *Gut.* 2017;66(1):70–78. doi:10.1136/gutjnl-2015-309800.
4. Routy B, Le Chatelier E, Derosa L, Duong CPM, Alou MT, Daillere R, Fluckiger A, Messaoudene M, Rauber C, Roberti MP, et al. Gut microbiome influences efficacy of PD-1-based immunotherapy against epithelial tumors. *Science.* 2018;359:91–97. doi:10.1126/science.aan3706.
5. Gopalakrishnan V, Spencer CN, Nezi L, Reuben A, Andrews MC, Karpinetz TV, Prieto PA, Vicente D, Hoffman K, Wei SC, et al. Gut microbiome modulates response to anti-PD-1 immunotherapy in melanoma patients. *Science.* 2018;359:97–103. doi:10.1126/science.aan4236.
6. Tanoue T, Morita S, Plichta DR, Skelly AN, Suda W, Sugiura Y, Narushima S, Vlamakis H, Motoo I, Sugita K, et al. A defined commensal consortium elicits CD8 T cells and anti-cancer immunity. *Nature.* 2019;565(7741):600–605. doi:10.1038/s41586-019-0878-z.
7. Coley WB. The Treatment of Inoperable Sarcoma by Bacterial Toxins (the Mixed Toxins of the Streptococcus erysipelas and the Bacillus prodigiosus). *Proc R Soc Med.* 1910;3:1–48.
8. Babjuk M, Burger M, Zigeuner R, Shariat SF, van Rhijn BW, Comperat E, Sylvester RJ, Kaasinen E, Bohle A, Palou Redorta J, et al. EAU guidelines on non-muscle-invasive urothelial carcinoma of the bladder: update 2013. *Eur Urol.* 2013;64:639–653. doi:10.1016/j.eururo.2013.06.003.
9. Su Y, Ortiz J, Liu S, Bugge TH, Singh R, Leppla SH, Frankel AE. Systematic urokinase-activated anthrax toxin therapy produces regressions of subcutaneous human non-small cell lung tumor in athymic nude mice. *Cancer Res.* 2007;67:3329–3336. doi:10.1158/0008-5472.CAN-06-4642.
10. Pastan I, Hassan R, Fitzgerald DJ, Kreitman RJ. Immunotoxin therapy of cancer. *Nat Rev Cancer.* 2006;6(7):559–565. doi:10.1038/nrc1891.
11. Kreitman RJ, Wilson WH, White JD, Stetler-Stevenson M, Jaffe ES, Giardina S, Waldmann TA, Pastan I. Phase

- I trial of recombinant immunotoxin anti-Tac(Fv)-PE38 (LMB-2) in patients with hematologic malignancies. *J Clin Oncol.* 2000;18(8):1622–1636. doi:10.1200/JCO.2000.18.8.1622.
12. Jimenez G, Urdiain M, Cifuentes A, Lopez-Lopez A, Blanch AR, Tamames J, Kampfer P, Kolsto AB, Ramon D, Martinez JF, et al. Description of *Bacillus toyonensis* sp. nov., a novel species of the *Bacillus cereus* group, and pairwise genome comparisons of the species of the group by means of ANI calculations. *Syst Appl Microbiol.* 2013;36:383–391. doi:10.1016/j.syapm.2013.04.008.
 13. Kantas D, Papatsiros VG, Tassis PD, Giavasis I, Bouki P, Tzika ED. A feed additive containing *Bacillus toyonensis* (Toyocerin((R))) protects against enteric pathogens in postweaning piglets. *J Appl Microbiol.* 2015;118:727–738. doi:10.1111/jam.12729.
 14. Santos FDS, Menegon YA, Piraine REA, Rodrigues PRC, Cunha RC, Leite FPL. *Bacillus toyonensis* improves immune response in the mice vaccinated with recombinant antigen of bovine herpesvirus type 5. *Benef Microbes.* 2018;9(1):133–142. doi:10.3920/BM2017.0021.
 15. Scharek-Tedin L, Pieper R, Vahjen W, Tedin K, Neumann K, Zentek J. *Bacillus cereus* var. *Toyo* modulates the immune reaction and reduces the occurrence of diarrhea in piglets challenged with *Salmonella Typhimurium* DT104. *J Anim Sci.* 2013;91(12):5696–5704. doi:10.2527/jas.2013-6382.
 16. Abdulmawjood A, Herrmann J, Riede S, Jimenez G, Becker A, Breves G. Evaluation of enterotoxin gene expression and enterotoxin production capacity of the probiotic strain *Bacillus toyonensis* BCT-7112T. *PLoS One.* 2019;14:e0214536. doi:10.1371/journal.pone.0214536.
 17. Turnbaugh PJ, Ley RE, Mahowald MA, Magrini V, Mardis ER, Gordon JL. An obesity-associated gut microbiome with increased capacity for energy harvest. *Nature.* 2006;444(7122):1027–1031. doi:10.1038/nature05414.
 18. Chung H, Pamp SJ, Hill JA, Surana NK, Edelman SM, Troy EB, Reading NC, Villablanca EJ, Wang S, Mora JR, et al. Gut immune maturation depends on colonization with a host-specific microbiota. *Cell.* 2012;149(7):1578–1593. doi:10.1016/j.cell.2012.04.037.
 19. Feng Q, Liang S, Jia H, Stadlmayr A, Tang L, Lan Z, Zhang D, Xia H, Xu X, Jie Z, et al. Gut microbiome development along the colorectal adenoma-carcinoma sequence. *Nat Commun.* 2015;6:6528. doi:10.1038/ncomms7528.
 20. Yahav S, Berkovich Z, Ostrov I, Reifen R, Shemesh M. Encapsulation of beneficial probiotic bacteria in extracellular matrix from biofilm-forming *Bacillus subtilis*. *Artif Cells Nanomed Biotechnol.* 2018;46(sup2):974–982. doi:10.1080/21691401.2018.1476373.
 21. Cao GT, Dai B, Wang KL, Yan Y, Xu YL, Wang YX, Yang CM. *Bacillus licheniformis*, a potential probiotic, inhibits obesity by modulating colonic microflora in C57BL/6J mice model. *J Appl Microbiol.* 2019;127(3):880–888. doi:10.1111/jam.14352.
 22. Zhao Y, Yuan L, Wan J, Sun Z, Wang Y, Sun H. Effects of potential probiotic *Bacillus cereus* EN25 on growth, immunity and disease resistance of juvenile sea cucumber *Apostichopus japonicus*. *Fish Shellfish Immunol.* 2016;49:237–242. doi:10.1016/j.fsi.2015.12.035.
 23. Kovac J, Miller RA, Carroll LM, Kent DJ, Jian J, Beno SM, Wiedmann M. Production of hemolysin BL by *Bacillus cereus* group isolates of dairy origin is associated with whole-genome phylogenetic clade. *BMC Genomics.* 2016;17(1):581. doi:10.1186/s12864-016-2883-z.
 24. Beecher DJ, Macmillan JD. Characterization of the components of hemolysin BL from *Bacillus cereus*. *Infect Immun.* 1991;59:1778–1784. doi:10.1128/IAI.59.5.1778-1784.1991.
 25. Jessberger N, Dietrich R, Schwemmer S, Tausch F, Schwenk V, Didier A, Martlbauer E. Binding to the target cell surface is the crucial step in pore formation of hemolysin BL from *Bacillus cereus*. *Toxins (Basel).* 2019;11(5):281. doi:10.3390/toxins11050281.
 26. Mathur A, Feng S, Hayward JA, Ngo C, Fox D, Atmosukarto II, Price JD, Schauer K, Martlbauer E, Robertson AAB, et al. A multicomponent toxin from *Bacillus cereus* incites inflammation and shapes host outcome via the NLRP3 inflammasome. *Nat Microbiol.* 2019;4(2):362–374. doi:10.1038/s41564-018-0318-0.
 27. Wang Q, Wang Y, Ding J, Wang C, Zhou X, Gao W, Huang H, Shao F, Liu Z. A bioorthogonal system reveals antitumour immune function of pyroptosis. *Nature.* 2020. doi:10.1038/s41586-020-2079-1.
 28. Gil M, Kim KE. Interleukin-18 is a prognostic biomarker correlated with CD8+ T cell and natural killer cell infiltration in skin cutaneous melanoma. *J Clin Med.* 2019;8(11):1993. doi:10.3390/jcm8111993.